

Electrochemical Detection of As(III) Ions in Hot Spring Water Based on a SiO₂-Au Nanocomposite

Feng Sun¹ and Guojing Fan^{2,*}

¹ School of Tourism and Land Resource, Chongqing Technology and Business University, Chongqing 400067, China.

² School of History Culture & Tourism, GanNan Normal University, Ganzhou 341000, Jiangxi, China

*E-mail: fanguojing890@163.com

Received: 3 June 2017 / Accepted: 15 August 2017 / Published: 12 September 2017

In this report, a SiO₂-Au nanohybrid was prepared for the detection of As(III) ions using an electrochemical strategy. The morphology and properties of the SiO₂-Au nanohybrid were characterized and analyzed via multiple techniques. Under optimized conditions, this nanohybrid material was utilized in the detection of As(III) in hot spring water samples collected from a tourist destination. The results suggested that an electrochemical sensor for the detection of As(III) could be used as a tool for the environmental protection of this tourist destination.

Keywords: As(III) ions; mesoporous silica; Gold; Electrochemical determination; Environmental protection

1. INTRODUCTION

As(III) ions are a highly toxic, relatively widespread water pollutant, and have harmed large numbers of people in many developing countries [1, 2]. A wide range of diseases, including stillbirth, heart disease, as well as lung, bladder, and skin cancer may arise from long-term exposure to As(III) ions [3-6]. There are two primary chemical forms of inorganic As(III), which are arsenate ions (i.e., HAsO₄⁻, H₂AsO₄, As^V, etc.), and the less common arsenite ions (i.e., H₃AsO₃, As^{III}, etc.), which are formed under more reducing conditions. Compared to arsenate ions, arsenite ions exhibit greater solubility in water and *ca.* 50 times higher toxicity, due to their ability to react with enzymes in the human respiratory system [7, 8]. The Bangladesh legal limit for the maximum concentration of As(III) ions in drinking water is 50 µg L⁻¹, but this value is only 10 µg L⁻¹ according to the recommendation of the World Health Organization (WHO) [9, 10].

Inductively coupled plasma mass spectrometry (ICP-MS) may be used to detect trace levels of As(III) ions in laboratory solutions, since this technique is remarkably sensitive, with a low limit of detection (LOD) in the nanomolar range [11-13]. Nevertheless, this technique suffers from the disadvantages of high cost and the inability to be used for field analysis. Therefore, the development of a sensitive and compact sensor for the detection of low concentrations of As(III) ions is critical.

Due to their excellent sensitivity, compactness, and ability to save time by generating reproducible assays, electrochemical techniques have been extensively explored for the detection of As(III) ions in previous reports. Thin silicate films have become widely used for the development of chemical sensors, since the response time is greatly reduced by their short diffusion path length [14, 15]. The sol-gel route [15] is a common technique for the preparation of fibres, hybrid materials, superfine powders, silicate films, etc. This route enables the cryochemical design and control of the microstructure of materials. The sol-gel route is characterized by lower temperatures, simplified conditions for manipulations, and a high homogeneity and purity of products [16]. A silica sol-gel film is typically prepared by the hydrolysis of alkoxy silane [17]. Nevertheless, it is difficult to control the preparation conditions to produce a sufficiently thin film. Therefore, the resulting film has poor conductivity, since the sol-gel silica is insulating. Another disadvantage is the poor mechanical behaviour caused by the degradation of the thick film during drying, as they are more likely to crack during the drying process than thin films.

In recent years, an electrochemical route has been developed to enhance the porosity of silicate films [18]. An electrode was introduced into an alkoxy silane-formed sol during its preparation. The silicate film immediately condenses on the surface of the electrode upon application of a sufficiently negative potential. It was observed that the electrochemically deposited film was tightly bound on the surface of the electrode, with its features maintained and tailored through the modification of electrodeposition parameters. Additionally, specific reagents could be added to the sol prior to electrodeposition, which then become entrapped in the film [19]. This technique results in the following characteristics: first, the film becomes more porous due to the independent drying and gelation processes. Second, it is easy to change the thickness of the film without the need for significant sol dilution. Third, this technique may have an application in bio-related fields, due to the remarkable reduction in methanol generated during the process. Finally, but perhaps most notably, the sol-gel-derived films could be prepared with increasing porosity by starting with sols that contain larger particles.

Due to their interface-dominated feature and high effective surface area, Au nanoparticles (Au NPs) exhibit excellent catalytic activity, as shown in several reports [20, 21]. The surface properties mentioned above have garnered substantial interest in analytical electrochemistry [22]. Au nanoparticles could be used as catalytic labels or electrochemical markers to form the conductive paths across electrodes, enabling the sensing of a wide variety of biomolecules [23]. Au nanoparticles could be stabilized in the silicate-based matrixes, which would modify the electrode to include edges well suited for electrochemical and catalytic applications. Furthermore, this route is convenient for the preparation and treatment of the solid films. The formation of Au NPs on the film could significantly enhance the activity in certain applications.

In this report, an Au-SiO₂ nanoparticle-decorated electrode was fabricated using HAuCl₄ and a tetraethylorthosilicate (TEOS) sol at -2.0 V. This sensor was found to be highly reliable and practical for the detection of As(III) ions without interfering effects, and even trace levels of As(III) ions could be detected with strong analytical signals.

2. EXPERIMENTS

2.1. Materials

The reduced form of nicotinamide adenine dinucleotide (NADH), nicotinamide adenine dinucleotide (NAD⁺), and alcohol dehydrogenase ADH (EC 1.1.1.1) from bakers yeast in the form of a lyophilized powder were purchased from Sigma. HAuCl₄·4H₂O and tetraethylorthosilicate were procured from Chemical Reagent Co., Ltd. All chemicals were of analytical reagent grade. All test solutions were prepared using ultrapure water obtained from a molecular water purification system. All measurements were performed at ambient temperature. A stock solution of As(III) (5 mM) was prepared by dissolving NaAsO₂ in aqueous HCl (0.1 M).

2.2. Characterizations

An EC 550 electrochemical workstation connected to an electrochemical cell containing a pH 7.0 phosphate buffer solution (10.0 mL) was used for electrochemical analysis. A typical three-electrode configuration was used, in which the working, reference, and auxiliary electrodes were a nano-Au/SiO₂ modified glassy carbon electrode (GCE), a saturated calomel electrode, and a Pt wire, respectively. Electrochemical impedance spectroscopy (EIS) experiments were carried out in a KCl solution (0.5 M) that contained K₄[Fe(CN)₆] / K₃[Fe(CN)₆] (2.0 mM) using a CHI 660C electrochemical workstation. X-ray photoelectron spectroscopy (XPS) was performed using a Kratos AXIS Nova (UK) spectrometer.

2.3. Preparation of nano-Au/SiO₂/GCE

After polishing with emery paper and an alumina slurry, the GCE was thoroughly rinsed with ultrapure water. The electrodes were then exposed to successive ultrasonication in nitric acid, ethanol and water, followed by drying at ambient temperature. Electrochemical treatment of a freshly polished electrode in a stirring mixture of 1.0% TEOS (H₂O: ethanol = 1:1) and 3.0 × 10⁻⁴ M HAuCl₄ for 20 s at -2.0 V yielded the Au/SiO₂ nanoparticle decorated glassy carbon electrode. The nano-Au/SiO₂ modified GCE was removed from the solution and thoroughly washed with ultrapure water, after which cyclic voltammetric scanning was performed for 20 consecutive cycles in a phosphate buffer solution (0 V - 0.80 V). The same procedure was performed for the preparation of nano-SiO₂ modified GCE with HAuCl₄.

3. RESULTS AND DISCUSSION

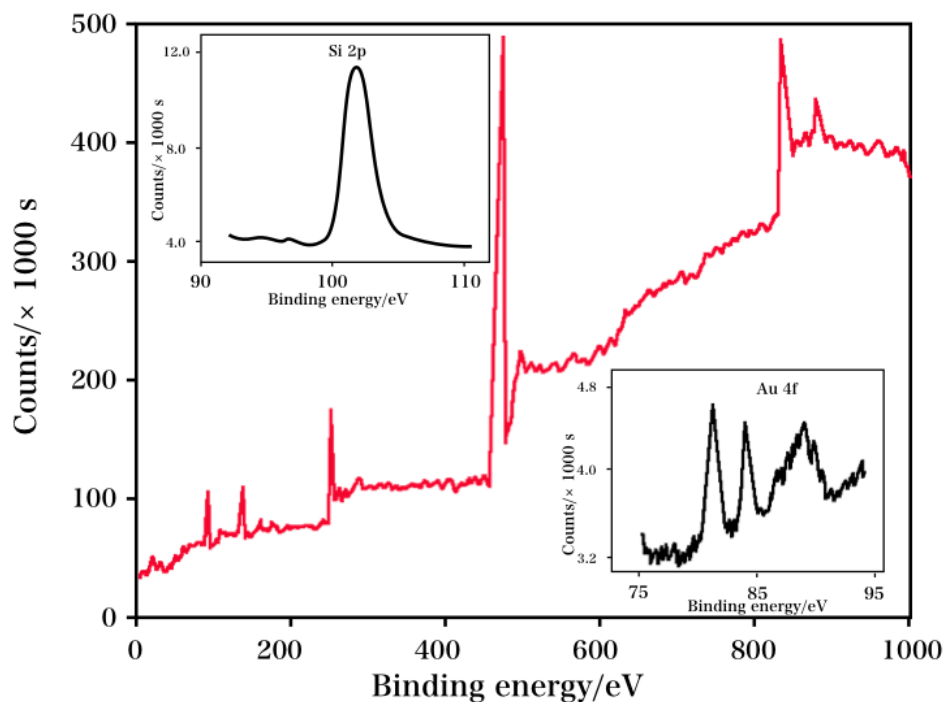


Figure 1. XPS profile of the surface of the nano-Au/SiO₂ modified GCE. Insets: XPS profile of Si 2p and Au 4f core levels.

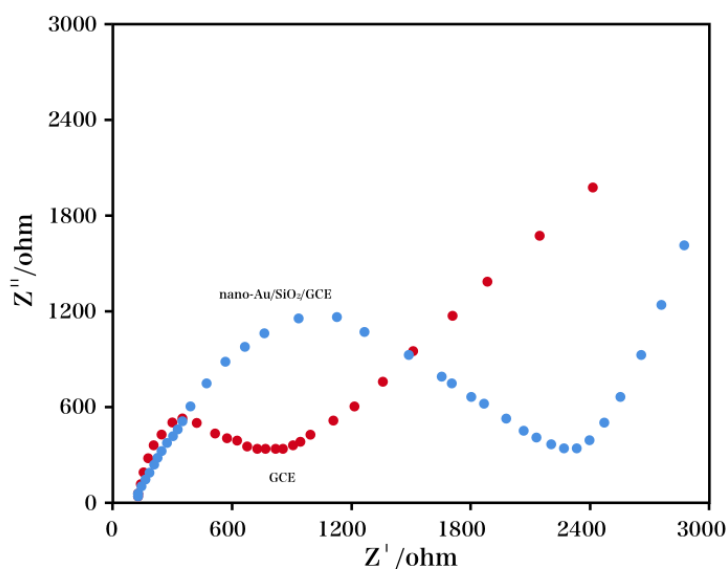


Figure 2. Nyquist plots for the original GCE and the nano-Au/SiO₂ modified GCE in a KCl solution (0.5 M) containing K₄[Fe(CN)₆]/K₃[Fe(CN)₆] (2.0×10^{-3} M).

XPS was used to analyze the surface composition of the nano-Au/SiO₂ modified GCE due to its high sensitivity for the measurement of the chemical composition and environment of the elements in materials. The elements on the surface of the electrode were detected by survey scans. Si 2p, O 1s, C

1s, and Au 4f core levels were observed, as shown in Fig. 1. The O 1s level and the Si 2p level were observed at 532.9 and *ca.* 103.6 eV, respectively, corresponding to the nano-SiO₂ matrix. The two peaks observed at 87.1 and 83.4 eV are attributed to Au 4f_{5/2} and 4f_{7/2}, at binding energies corresponding to Au⁰. From these results, we can conclude that the Au/SiO₂ composite nanoparticles have been electrochemically deposited on the glassy carbon electrode surface [24, 25].

The interfacial features of electrodes are typically investigated by EIS. The electron transfer kinetics of the redox probe at the electrode interface were controlled by the electron transfer resistance (Ret), represented by the diameter of the semicircle. It can also provide information regarding the change in impedance at the interface between the electrode surface and electrolyte solution [26, 27]. The original GCE and the nano-Au/SiO₂ modified GCE were placed in a mixture of K₄[Fe(CN)₆]/K₃[Fe(CN)₆] (2.0×10^{-3} M) and KCl solution (0.5 M) and were characterized via the Nyquist plots in Fig. 2. The nano-Au/SiO₂ modified GCE exhibited remarkably decreased resistance for the charge transfer than the original GCE. Based on these results, the Au/SiO₂ nanoparticles were shown to be an effective conduction medium by connecting the electrolyte solution and the electrode surface via large numbers of electroactive sites.

The behaviour of the nano-Au/SiO₂ modified GCE was initially investigated by CV measurements in HCl (0.1 M) in the presence of As(III) solution (0.5 mM), in the potential range from -0.5 to 0.5 (vs. SCE, 100 mV/s). The current densities of the Au electrode and the original GCE were recorded and compared. No significant response to As(III) ions was observed when using the original GCE, as shown in Fig. 3. A reduction peak was observed *ca.* -0.25 V when using the Au electrode or the nano-Au/SiO₂ modified GCE, as shown in their curves, corresponding to the 3 electron reduction of As(III) to As(0) [28].

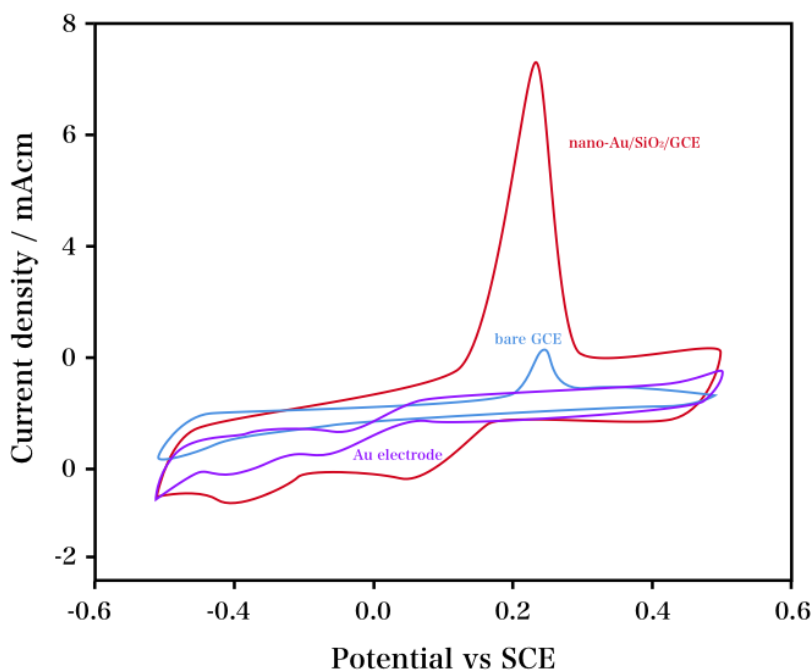


Figure 3. CV characterization of As(III) (0.5 mM) in HCl solution (0.1 M) at the nano-Au/SiO₂ modified GCE, the original GCE and Au electrode. Scan rate: 100 mV/s.

A greater oxidation peak was recorded at 0.15 V on the reverse scan, corresponding to the reoxidation of As(0) on the Au surface back to its original +3 oxidation state. The nano-Au/SiO₂ modified GCE was much more sensitive to As(III) than the Au macrodisc electrode, as indicated in Fig. 3.

Square wave voltammetry (SWV) and linear sweep voltammetry (LSV) measurements were performed in order to study the performance of the AuCNTs modified electrode for the detection of As(III) ions in water. Measurements were taken using an optimized system based on that developed by Dai et al. [29], with 0.1 M HCl as the supporting electrolyte. For the nano-Au/SiO₂ composite, As(III) was deposited at an optimal scan rate of 100 mV/s, with a deposition time of 60, 120 and 240 s using SWV, and 60, 120, 180, and 240 s using LSV [29]. The size of the stripping peak increased with the deposition time and the concentration of nano-Au/SiO₂ composite on the electrode surface for both LSV and SWV, with SWV as the more sensitive technique (Fig. 4). Nevertheless, SWV was more sensitive at the nano-Au/SiO₂ modified GCE, whereas the LOD was much lower due to the absence of such problem.

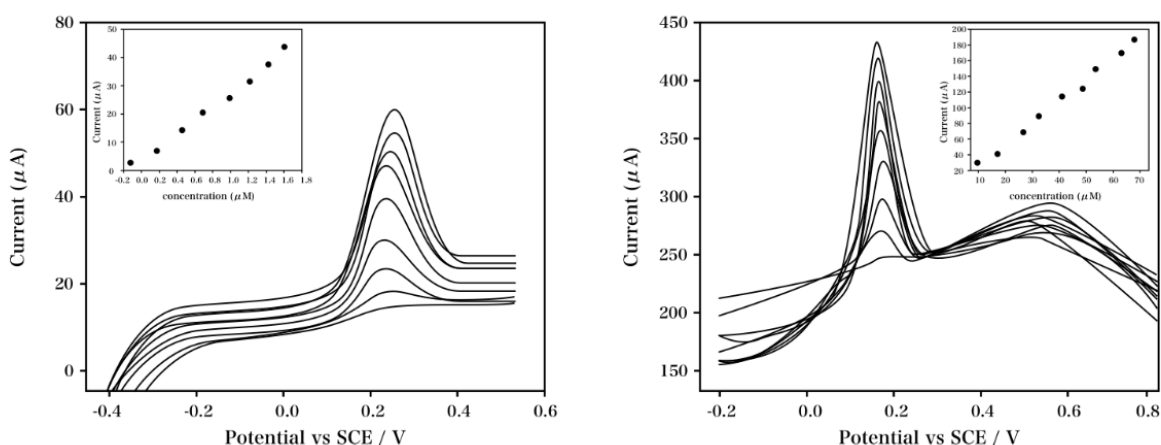


Figure 4. (A) LSV and (B) SWV of a standard addition plot of nano-Au/SiO₂ modified GCE in HCl (0.1 M). Parameters for LSV: pre-deposition at -0.4 V (vs. SCE) for 240 s at a scan rate of 100 mV/s; Parameters for SWV: pre-deposition at -0.4 V (vs. SCE) for 120 s, $\Delta E_s = 2$ mV, $E_{sw} = 20$ mV, $f = 50$ Hz. Inset: plot of peak height vs. the arsenic concentration.

Table 1. Comparison of As(III) detection by the proposed method and those of other reports.

Electrode	LDR (µg/L)	LOD (µg/L)	Reference
Ultra-thin graphene oxide nanosheets	0.7-11	0.5	[30]
Carbon paste electrode	5-40	1.408	[31]
Organo-modified sericite	0.4-66	0.1	[32]
Graphene paste-TTCN-AuNPs	0.2-17	0.05	[33]
Zirconia nanocubes	5-60	1.47	[34]
nano-Au/SiO ₂ /GCE	0.1-40	0.07	This work

The electrochemical response for the deposition of As(III) on the nano-Au/SiO₂ modified GCE was measured using SWV and LSV and compared, with optimal deposition times of 120 s and 240 s for SWV and LSV, respectively (Fig. 4). Compared to a previous report on a gold nanoparticle modified GC electrode by Dai et al. [29], SWV provides much higher sensitivity, but a low LOD due to the high level of noise generated in the baseline.

Repeated calibration tests were performed with SWV and LSV at a potential of -0.4 V (vs. SCE), and the optimal deposition times were 120 s and 240 s for SWV and LSV, respectively. For SWV measurements, the LOD was calculated to be 0.07 $\mu\text{g/L}$, and the linear detection range was $0.1 - 40$ $\mu\text{g/L}$. For LSV measurements, the LOD was calculated to be 0.63 $\mu\text{g/L}$ (S/N=3), and the linear detection range was $1 - 40$ $\mu\text{g/L}$. Table 1 compares our proposed As(III) sensor to other electrochemical sensors. Compared to other electrochemical sensors, the nano-Au/SiO₂ modified GCE exhibited a similar linear detection range for the As(III) LOD. Additionally, our sensor was found to have significant reproducibility. After repeated As(III) detection for eight trials, reproducible current responses were recorded, with a relative standard deviation (RSD) of 1.14%. Therefore, the nano-Au/SiO₂ modified GCE is potentially suitable for the detection of As(III) in environmental samples.

The application of the nano-Au/SiO₂ modified GCE for the detection of As(III) in environmental samples was studied by using two hot spring water samples collected from a tourist destination in Gannan, and analysing them according to the procedures used in the laboratory. Table 2 displays the concentration of As(III) in various environmental samples. The nano-Au/SiO₂ modified GCE exhibited excellent performance for the detection of As(III) in four test environmental samples. Combined with a pre-test evaluation, the nano-Au/SiO₂ modified GCE was found to be suitable as a compact electrochemical sensor for on-site environmental protection applications.

Table 2. The detection of As(III) in hot spring water specimens using the nano-Au/SiO₂/GCE.

Sample	Added ($\mu\text{g/L}$)	Found ($\mu\text{g/L}$)	Recovery (%)
Sample 1	0	0	—
	10	10.07	100.7
Sample 2	0	0	—
	15	14.95	99.67
Sample 1	0	0	—
	20	20.14	100.7
Sample 2	0	0	—
	30	30.50	101.67

4. CONCLUSIONS

In this report, a nano-Au/SiO₂ modified GCE was fabricated using a one-step strategy. This nanohybrid material was used for the electrochemical detection of As(III). The LOD was calculated to be 0.07 $\mu\text{g/L}$, with a linear detection range of $0.1 - 40$ $\mu\text{g/L}$. Furthermore, this electrochemical sensor was successfully used to detect As(III) in real environmental water samples.

ACKNOWLEDGEMENT

This study was supported by a grant from the Science and technology research of Chongqing Municipal Education Commission (No. KJ1500638).

References

1. M. Arienzo, P. Adamo, J. Chiarenzelli, M. Bianco and A. De Martino, *Chemosphere*, 48 (2002) 1009.
2. X. Zhang, T. Zeng, C. Hu and S. Hu, *Analytical Methods*, 8 (2016) 1162.
3. J. Luong, E. Lam and K. Male, *Analytical Methods*, 6 (2014) 6157.
4. B. Zhang, J. Liu, X. Ma, P. Zuo, B. Ye and Y. Li, *Biosensors and Bioelectronics*, 80 (2016) 491.
5. A. Salimi, N. Amini, K. Naderi and H. Ghafuori, *Journal of Molecular Liquids*, 233 (2017) 100.
6. M. Yang, X. Chen, T. Jiang, Z. Guo, J. Liu and X. Huang, *Anal. Chem.*, 88 (2016) 9720.
7. S. Radić, H. Crnojević, V. Vujčić, G. Gajski, M. Gerić, Ž. Cvetković, C. Petra, V. Garaj-Vrhovac and V. Oreščanin, *Science of the Total Environment*, 543 (2016) 147.
8. S. Toor, P. Devi and B. Bansod, *Aquatic Procedia*, 4 (2015) 1107.
9. J. Jeong, J. Das, M. Choi, J. Jo, M. Aziz and H. Yang, *The Analyst*, 139 (2014) 5813.
10. M. Yang, Z. Guo, L. Li, Y. Huang, J. Liu, Q. Zhou, X. Chen and X. Huang, *Sensors and Actuators B: Chemical*, 231 (2016) 70.
11. B. Klaue and J. Blum, *Anal. Chem.*, 71 (1999) 1408.
12. V. Gomez and M. Callao, *TrAC Trends in Analytical Chemistry*, 25 (2006) 1006.
13. D. Hung, O. Nekrassova and R. Compton, *Talanta*, 64 (2004) 269.
14. A. Khramov and M. Collinson, *Chemical Communications*, (2001) 767.
15. J. Li, L. Chia, N. Goh and S. Tan, *Journal of Electroanalytical Chemistry*, 460 (1999) 234.
16. L. Hench and J. West, *Chemical Reviews*, 90 (1990) 33.
17. B. Wang, B. Li, Q. Deng and S. Dong, *Anal. Chem.*, 70 (1998) 3170.
18. R. Shacham, D. Avnir and D. Mandler, *Adv. Mater.*, 11 (1999) 384.
19. M. Collinson, N. Moore, P. Deepa and M. Kanungo, *Langmuir*, 19 (2003) 7669.
20. A. Yu, Z. Liang, J. Cho and F. Caruso, *Nano Letters*, 3 (2003) 1203.
21. J. Wang, *Small*, 1 (2005) 1036.
22. L. Tang, G. Zeng, G. Shen, Y. Li, Y. Zhang and D. Huang, *Environmental Science & Technology*, 42 (2008) 1207.
23. X. Mao, J. Jiang, Y. Luo, G. Shen and R. Yu, *Talanta*, 73 (2007) 420.
24. A. Schlather, A. Manjavacas, A. Lauchner, V.S. Marangoni, C. DeSantis, P. Nordlander and N.J. Halas, *The Journal of Physical Chemistry Letters*, 8 (2017) 2060.
25. J. Montaño-Priede, J. Coelho, A. Guerrero-Martínez, O. Peña-Rodríguez and U. Pal, *The Journal of Physical Chemistry C*, 121 (2017) 9543.
26. C. Zheng, L. Liang, S. Xu, H. Zhang, C. Hu, L. Bi, Z. Fan, B. Han and W. Xu, *Analytical and Bioanalytical Chemistry*, 406 (2014) 5425.
27. J. Liu, C. Kan, B. Cong, H. Xu, Y. Ni, Y. Li and D. Shi, *Plasmonics*, 9 (2014) 1007.
28. T. Loučka, *Journal of Electroanalytical Chemistry and Interfacial Electrochemistry*, 47 (1973) 103.
29. X. Dai, O. Nekrassova, M. Hyde and R. Compton, *Analytical Chemistry*, 76 (2004) 5924.
30. S. Kumar, G. Bhanjana, N. Dilbaghi, R. Kumar and A. Umar, *Sensors and Actuators B: Chemical*, 227 (2016) 29.
31. D. Tiwari, Zirlianggura and S. Lee, *Journal of Electroanalytical Chemistry*, 784 (2017) 109.
32. M. Kim, J. Yang, Y. Park, I. Lee, K. Min, C. Jeon and S. Lee, *Environmental Science and Pollution Research*, 23 (2016) 1044.

33. B. Sanghavi, N. Gadhari, P. Kalambate, S. Karna and A. Srivastava, *Microchim. Acta.*, 182 (2015) 1473.
34. G. Bhanjana, N. Dilbaghi, S. Chaudhary, K. Kim and S. Kumar, *The Analyst*, 141 (2016) 4211.

© 2017 The Authors. Published by ESG (www.electrochemsci.org). This article is an open access article distributed under the terms and conditions of the Creative Commons Attribution license (<http://creativecommons.org/licenses/by/4.0/>).